ACADEMIC PRESS

Available online at www.sciencedirect.com

SCIENCE DIRECT®

DEVELOPMENTAL BIOLOGY

Developmental Biology 253 (2003) 279–290

www.elsevier.com/locate/ydbio

Formation of the digestive system in zebrafish. I. Liver morphogenesis

Holly A. Field,[a] Elke A. Ober,[a] Tobias Roeser,[b] and Didier Y.R. Stainier[a,*]

[a] *Department of Biochemistry and Biophysics, Programs in Developmental Biology, Genetics and Human Genetics, University of California, San Francisco, San Francisco, CA 94143, USA*

[b] *Department of Physiology, University of California, San Francisco, San Francisco, CA 94143, USA*

Received for publication 21 August 2002, revised 8 October 2002, accepted 8 October 2002

Abstract

Despite the essential functions of the digestive system, much remains to be learned about the cellular and molecular mechanisms responsible for digestive organ morphogenesis and patterning. We introduce a novel zebrafish transgenic line, the gutGFP line, that expresses GFP throughout the digestive system, and use this tool to analyze the development of the liver. Our studies reveal two phases of liver morphogenesis: budding and growth. The budding period, which can be further subdivided into three stages, starts when hepatocytes first aggregate, shortly after 24 h postfertilization (hpf), and ends with the formation of a hepatic duct at 50 hpf. The growth phase immediately follows and is responsible for a dramatic alteration of liver size and shape. We also analyze gene expression in the developing liver and find a correlation between the expression of certain transcription factor genes and the morphologically defined stages of liver budding. To further expand our understanding of budding morphogenesis, we use loss-of-function analyses to investigate factors potentially involved in this process. It had been reported that *no tail* mutant embryos appear to lack a liver primordium, as assessed by *gata6* expression. However, analysis of gutGFP embryos lacking Ntl show that the liver is in fact present. We also find that, in these embryos, the direction of liver budding does not correlate with the direction of intestinal looping, indicating that the left/right behavior of these tissues can be uncoupled. In addition, we use the *cloche* mutation to analyze the role of endothelial cells in liver morphogenesis, and find that in zebrafish, unlike what has been reported in mouse, endothelial cells do not appear to be necessary for the budding of this organ.

Keywords: Endoderm; Hepatocytes; Chirality; *cloche*

Introduction

The digestive system consists of an alimentary canal and its associated organs, the liver, gallbladder, and pancreas. Although pancreas development has received a lot of attention in different organisms (Biemar et al., 2001; Edlund, 2002; Slack, 1995), formation of the liver is relatively understudied. Hepatocytes make up the majority of the liver and carry out most of the liver's function, including bile production, blood detoxification, the production of critical plasma proteins and clotting factors, and the storage of many substances, such as lipids, amino acids, iron, and glycogen. The liver develops as an outgrowth of the anterior intestine. Tissue explant studies have demonstrated the necessity of adjacent mesoderm for hepatocyte differentiation and maintenance (Cascio and Zaret, 1991; Gauldi et al., 1996; Le Douarin, 1970, 1975). More recent studies have implicated FGFs (Jung et al., 1999) as well as BMPs (Rossi et al., 2001) in these tissue interactions (reviewed by Zaret, 2002). Although the molecular details of hepatocyte differentiation are beginning to emerge, much remains to be learned. Even less is known about the mechanisms responsible for liver morphogenesis. For example, while *Prox1* is known to be necessary for the migration of hepatocytes into the septum transversum in mouse (Sosa-Pineda et al., 2000), its specific mechanism of action remains to be determined.

The zebrafish has emerged as a valuable organism for genetic studies of vertebrate organ formation and promises to be a significant addition to the model organisms currently

* Corresponding author. Department of Biochemistry and Biophysics, HSE 1530C, Box 0448, 513 Parnassus Ave., San Francisco, CA 94143-0448. Fax: +1-415-476-3892.

E-mail address: didier_stainier@biochem.ucsf.edu (D.Y.R. Stainier).

0012-1606/03/$ – see front matter © 2003 Elsevier Science (USA). All rights reserved.
PII: S0012-1606(02)00017-9

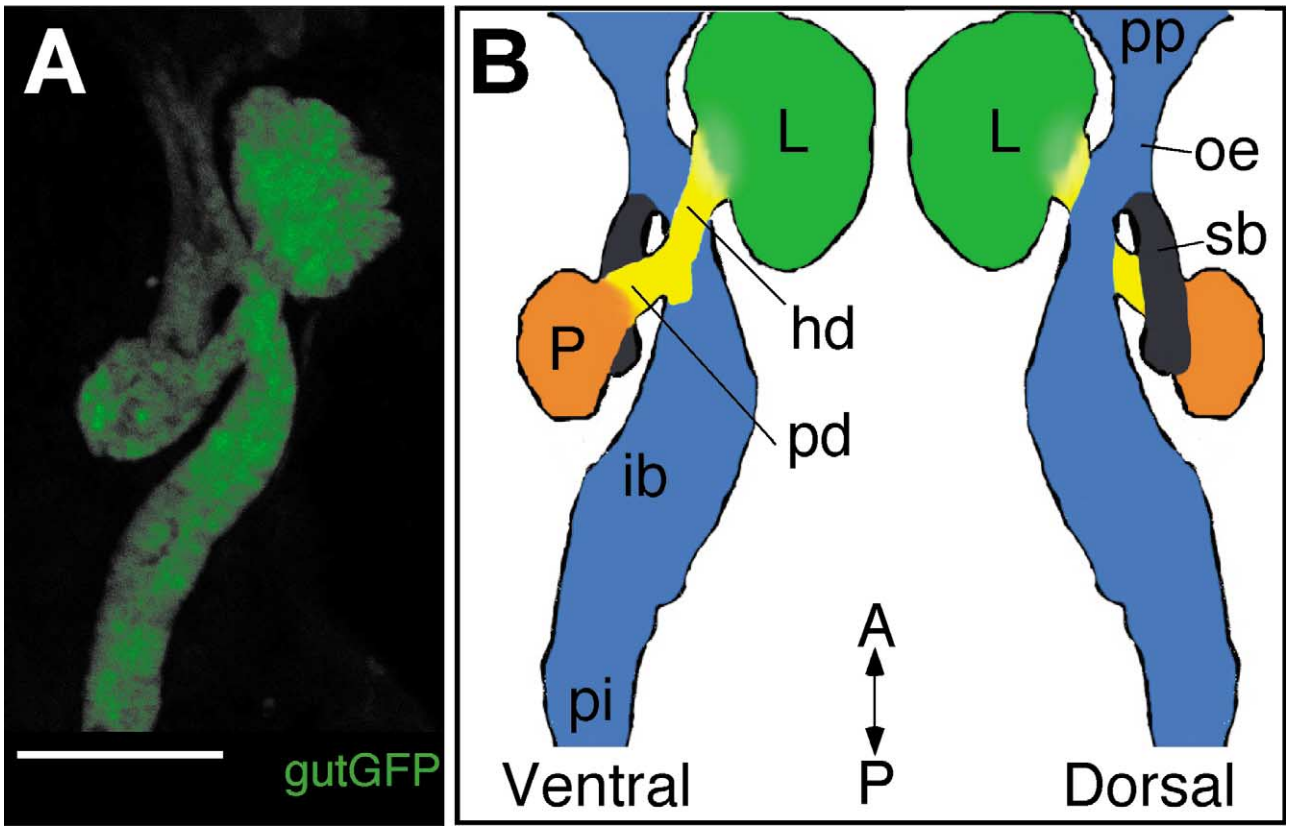

Fig. 1. The 52-hpf zebrafish digestive system as visualized in the stable transgenic gutGFP line. (A) Two-dimensional projection of a confocal stack, ventral view with anterior to the top. GFP expression occurs in all organs of the digestive system as well as the endodermal lining of the swim bladder. Scale bar, 100 μm. (B) Schematic drawings (ventral and dorsal views, anterior to the top) showing the identity and location of GFP-expressing organs at 52 hpf. L, liver; hd, hepatic duct; pd, pancreatic duct; P, pancreas; ib, intestinal bulb; pi, posterior intestine; pp, posterior region of the pharynx; oe, oesophagus; sb, swim bladder.

used to study liver development. Since the liver is an early hematopoietic organ in mammals, mutations affecting its development in mouse lead to early lethality from anemia (Reimold et al., 2000), thus making prolonged in vivo studies of mouse liver morphogenesis difficult. Hematopoiesis in zebrafish takes place in the intermediate cell mass (ICM) and subsequently in the kidney, not the liver (reviewed by Thisse and Zon, 2002), thus liver defects do not lead to anemia. In addition, zebrafish embryos lacking circulation receive enough oxygen through diffusion to allow embryonic development to proceed relatively normally for several days (reviewed by Stainier, 2001), eliminating some of the problems encountered with mammalian model organisms. The relative optical clarity of zebrafish embryos is another advantage for studies of internal organs, especially in conjunction with the use of GFP transgenes, which allow analysis of fluorescing tissues throughout development in the living embryo.

Here, we introduce a transgenic zebrafish line, the gutGFP line, that expresses GFP throughout the developing

Fig. 2. Time course of liver budding. (A–F) Two-dimensional projections of confocal stacks showing ventral views of the gutGFP line, anterior to the top. Scale bar, 100 μm. Embryos were fixed and imaged at (A) 24, (B) 28, (C) 30, (D) 34, (E) 36, and (F) 46 hpf. (A, B) The liver (arrowhead) starts budding from the intestinal rod between 24 and 28 hpf. (C) At 30 hpf, the liver is a smooth thickening on the outer curvature of the intestinal bulb primordium, which at this time has a clear leftward bend. (D) A furrow (open arrow) begins to form between the medial anterior edge of the liver and the adjacent oesophagus and continues to expand posteriorly (E, F) to separate the liver from the intestinal bulb primordium. The pancreas (asterisk) and endodermal lining of the swim bladder (arrow) can also be seen developing from the intestinal bulb primordium over time. (G–I) Transverse sections through the gutGFP line stained with rhodamine-labeled phalloidin to visualize surrounding tissues. The liver is marked by an arrowhead; the intestinal bulb primordium is outlined in white. Dorsal is to the top, and left is to the right to keep with the orientation of the ventral views. The level of the sections in (G–I) is indicated by the yellow dashed lines in (B), (C), and (E), respectively. (G) At 28 hpf, the first aggregation of hepatocytes from the intestinal bulb primordium is slightly to the left of the midline and adjacent to the yolk (y). The tissue that resides between the endoderm and the overlying notochord and somites is the lateral plate mesoderm. (H) At 30 hpf, the budding liver, which is positioned left of the midline, has an extensive connection to the intestinal bulb primordium. Lateral plate mesoderm is present both dorsal and ventral to the intestinal bulb primordium, but not ventral to the liver. (I) By 36 hpf, the connection between the liver and intestinal bulb primordium has started to restrict, and lateral plate mesoderm is present in the resulting space. The liver sits directly on the yolk (y). n, notochord; s, somites; nt, neural tube.

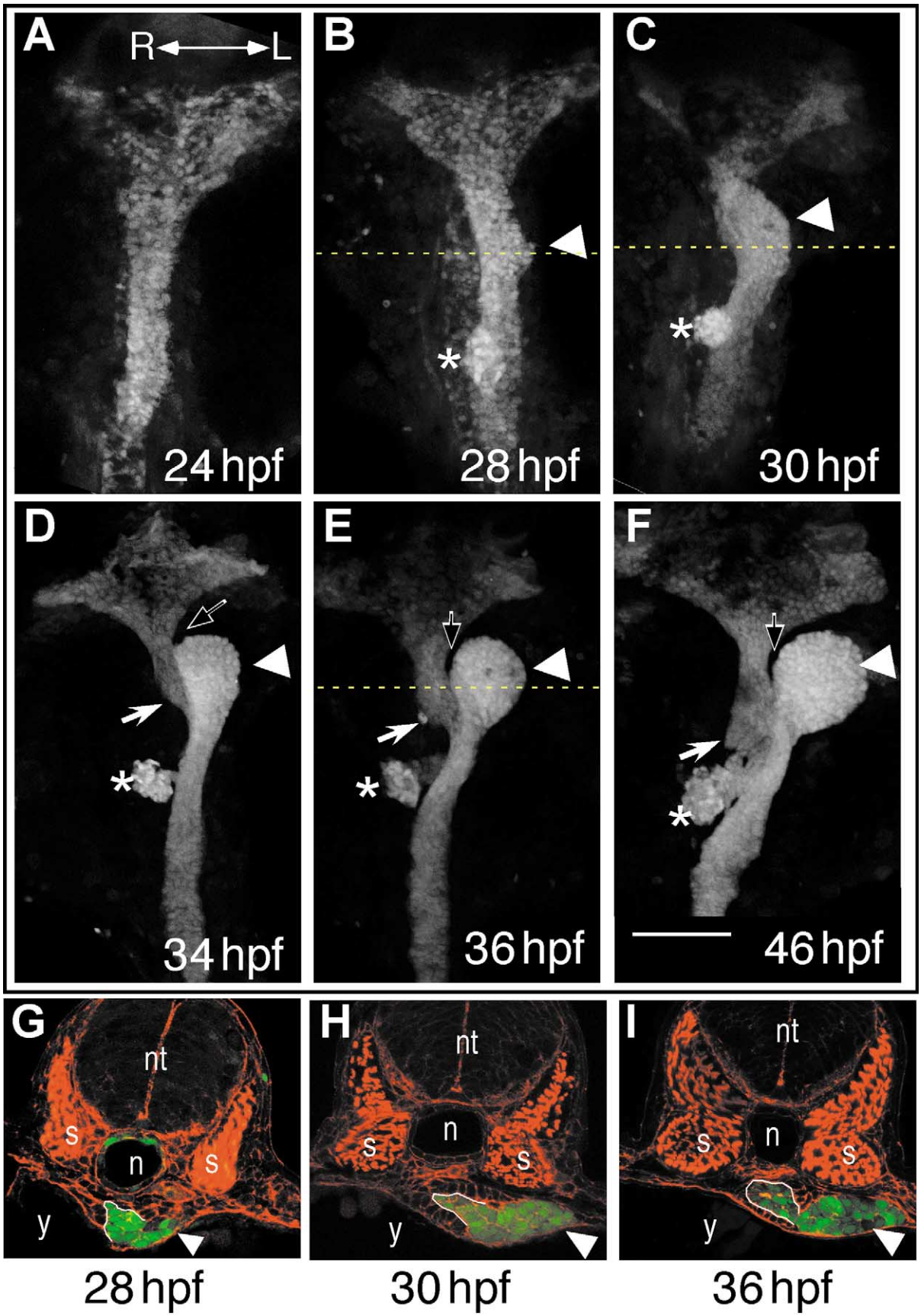
A
R
L
24 hpf
B
28 hpf
C
30 hpf
D
34 hpf
E
36 hpf
F
46 hpf
G
nt
s
n
s
y
28 hpf
H
nt
n
s
s
y
30 hpf
I
nt
n
s
s
y
36 hpf

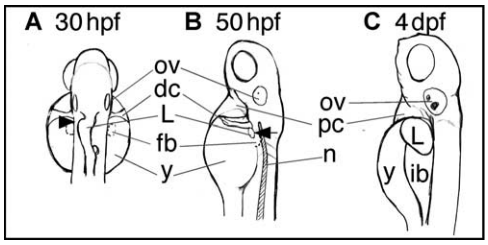

Fig. 3. Sketches showing the location of the liver in the context of the embryo at 30 hpf (A), 50 hpf (B), and 4 dpf (C). (A, B) At 30 and 50 hpf, the liver (arrowhead) extends from the duct of Cuvier, anteriorly, to the midlevel of the fin bud, posteriorly. (C) At 4 dpf, the liver can be seen touching the pericardial cavity and resting on top of the remaining yolk. The intestinal bulb has inflated and is pressed against the left side of the embryo. ov, otic vesicle; dc, duct of Cuvier; L, liver; fb, fin bud; y, yolk; ib, intestinal bulb; n, notochord; pc, pericardial cavity.

digestive system. This unique tool can be used to examine, in living and fixed embryos, endodermal organs otherwise obscured by the yolk ball and dorsal tissues. In the present study, we investigate liver morphogenesis both in wildtype and in a selective and informative set of mutant embryos. Our analyses reveal the timing and nature of the morphogenetic movements, as well as gene expression patterns, associated with liver budding. We also find that directional outgrowth of the liver can be uncoupled from the direction of intestinal looping, and that, surprisingly and contrary to what has been reported in mouse (Matsumoto et al., 2001), endothelial cells do not appear to be required for budding morphogenesis of the liver in zebrafish.

Materials and methods

Embryo culture and zebrafish stocks

Fish and embryos were maintained, collected, and staged as described (Westerfield, 1995). We collected embryos homozygous for the *clo*^{s5} mutation (Wayne Liao and D.Y.R.S., unpublished observations) and used wildtype siblings as controls.

Transgenic animals

To visualize the gut and associated organs, we used a new stable transgenic strain referred to as the gutGFP line. This line was generated by Tobias Roeser in Herwig Baier's group in the lab of Christiane Nüsslein-Volhard (Tübingen, Germany), using a DNA construct that consists of a *Xenopus EF-1α* promoter regulating GFP expression. Characterization of the inserted transgene and the insertion site is ongoing and will be published elsewhere. The gutGFP line will be available through the Zebrafish Stock Center.

To visualize endothelial cells, we used a stable transgenic line that expresses GFP under the control of the mouse *Tie2* enhancer (Motoike et al., 2000).

RNA in situ localization

In situ hybridization was performed with digoxigenin-labeled RNA anti-sense probes for the following genes: *foxA2/axial/hnf3β, foxA3/fkd2* (Odenthal and Nüsslein-Volhard, 1998), *prox1* (Glasgow and Tomarev, 1998), *selenoprotein Pb (sePb)* (Kryukov and Gladyshev, 2000; Kudoh et al., 2001), *hnf4* (Kudoh et al., 2001), and *sox17* (Alexander and Stainier, 1999).

Whole-mount in situ hybridization was performed as described (Alexander et al., 1998) with the following modifications. Embryos older than 24 hpf were raised in 0.003% 1-phenyl-2- thiourea (PTU; Sigma) in egg water to inhibit the production of pigment and, after fixation, were treated with 10 μg/ml proteinase K (Roche Diagnostics).

Images were acquired by using either a Zeiss StemiSV11 stereomicroscope or a Zeiss Axioplan, equipped with a Zeiss color Axiocam digital camera running Axiovision 3.0 software.

Immunofluorescence and histological stains

Immunofluorescent analysis of protein expression was performed with a rabbit anti-Prox 1 antibody (Wigle et al., 1999). Embryos were fixed in 4% paraformaldehyde for 1 h at room temperature, then manually deyolked, washed with PBS, and incubated in a 1:100 dilution of antibody in PBS with 1% Triton-X and 2% sheep serum for approximately 40 h at 4°C. Embryos were mounted in 4% SeaPlaque agarose (BioWhittaker Molecular Applications) in PBS. Bound antibody was detected on transverse vibratome sections (100 μm thick) by using Alexa Fluor-594 goat anti-rabbit IgG H + L antibody (1:200; Molecular Probes). To visualize actin, transverse vibratome sections were incubated in rhodamine-labeled phalloidin (1:100; Molecular Probes).

Confocal images were acquired by using a Leica TCS NT confocal microscope. Image overlays were assembled by using Adobe Photoshop 5.0 LE. Two-dimensional projections were generated by using Scion Image version 4.0.2.

Morpholino injection

We designed morpholino oligonucleotides to overlap the translational start site of *no tail*, 5′-GACTTGAGGCAG-G**CAT**ATTTCCGAT-3′, and they were injected essentially as described (Heasman et al., 2000). Briefly, morpholinos were solubilized in 10 mM Hepes, pH 7.6, to create a 1 mM stock. Stock was diluted with a 5 mM Hepes, pH 7.6, solution that contained 0.05% phenol red for visual detection of successfully injected embryos. A total of 3.2 ng of morpholino was injected per embryo. Noninjected, Hepes-injected, and embryos injected with morpholinos designed against other genes served as controls.

Results

Introduction of the gutGFP line

To investigate liver development in zebrafish, we used a novel GFP-expressing transgenic line which facilitates observation of the digestive tract and its associated organs in living (data not shown) as well as fixed embryos (Fig. 1A). This gutGFP line was generated by random integration of a GFP-containing construct (see Materials and methods). Initially ubiquitous, GFP expression becomes restricted to the endoderm by approximately 22 hpf. Expression is also observed in the notochord until approximately 30 hpf, and in the eye and hatching gland (data not shown). GFP expression is sometimes variable in heterozygous animals (data not shown) but uniform throughout the endoderm of embryos homozygous for the transgene. Homozygous animals are viable and have no observable phenotype.

At 52 hpf, when the internal organs are easily recognizable, GFP expression is present along the entire alimentary canal: the pharynx, oesophagus, intestinal bulb, and the posterior intestine up to and including the anus (Fig. 1B). Additionally, expression is observed in the endodermal component of all accessory organs: the liver, pancreas, gall bladder (visible by 72 hpf; data not shown), the duct systems of these organs, and the swim bladder (Fig. 1B).

Liver morphogenesis

To characterize the progression of liver morphogenesis, we analyzed the pattern of GFP expression in homozygous gutGFP embryos at multiple time points between 24 and 46 hpf. We describe liver morphogenesis in two phases: (1) budding, which is further divided into three stages based on distinct liver morphology, and (2) growth. Confocal analysis of 24-hpf embryos revealed the endoderm as a flat sheet in the pharyngeal region that constricts into a solid rod of midline cells, the intestinal rod, just rostral to the first somite (Fig. 2A). By 28 hpf, two thickened regions are present on the intestinal rod (Fig. 2B). The posterior thickening, situated dorsally on the intestinal rod at the level of the fourth somite, expresses Somatostatin and will contribute to the pancreas (unpublished observations). The anterior thickening is positioned slightly left of the midline and projects from the ventral side of the rod at the level of the first somite. This aggregation of cells marks the first morphogenetic movements of liver organogenesis and is defined as budding stage I. The timing of this first stage of budding varies slightly, but was consistently seen between 24 and 28 hpf.

During stage II, the intestinal bulb primordium undergoes a leftward bend at the level of the developing liver. The aggregate of liver cells increases in size, resulting in a smooth, thickened area along the outer curvature of the intestinal bulb primordium by 30 hpf (Fig. 2C). We define this process as budding stage II, since the appearance of the nascent liver is distinct from that observed in stage I (Fig. 2C and D).

Stage III of budding begins at approximately 34 hpf when a furrow starts to form between the liver bud and the adjacent oesophagus (Fig. 2E). This furrow expands posteriorly over time, restricting the connection between the liver and the intestinal bulb primordium (Fig. 2E and F). By 50 hpf, cells connecting these two organs have formed the hepatic duct. Transverse sections through the hepatic duct at this time show between 5 and 10 cells, with pronounced apical actin staining, arranged around a small central lumen to form a simple tubular duct (data not shown). Hepatic duct formation marks the end of stage III and the end of the budding process.

Upon completion of budding, the liver is a well-defined structure that increases in size and modifies its shape and placement. We refer to this subsequent size increase as the growth phase of liver development. By 72 hpf, the size of the liver has increased moderately but the shape has not altered. By 96 hpf, liver growth has resulted in a medial expansion so that it extends from the left side of the embryo all the way across the midline ventral to the oesophagus (data not shown).

During budding, hepatocytes emerge from the intestinal rod and protrude to the left as a disorganized but cohesive mass of cells (Fig. 2G–I). The hepatocytes maintain very close apposition with one another as the liver expands to the left. Throughout the budding phase, mesodermal cells are observed adjacent to the intestine and dorsal to the liver (Fig. 2G–I). As the furrow between the liver and oesophagus expands, mesodermal cells can be seen in the resulting gap (Fig. 2I). The liver is directly adjacent to the yolk ball, and we observed no mesodermal cells in contact with the ventral face of the liver at any stage of liver budding (Fig. 2G–I). The necessity of adjacent mesoderm on liver development has been shown in other vertebrates (Cascio and Zaret, 1991; Gauldi et al., 1996; Le Douarin, 1970, 1975), but in zebrafish, the influence of surrounding tissues has never been studied. The proximity of the developing liver to the yolk and mesoderm makes these tissues likely candidates to be involved in the budding process.

In addition to investigating the location of the liver with respect to adjacent tissues, it is important to note the position of the liver with respect to the entire embryo. During budding, the anterior edge of the liver aligns with the duct of Cuvier and extends caudally to the mid-level of the fin bud (Fig. 3A). By the completion of the budding process at 50 hpf, the liver protrudes slightly beyond the lateral edge of the left somites. A left lateral view shows its anterior edge situated immediately posterior to the duct of Cuvier and its posterior edge extending halfway through the level of the fin bud (Fig. 3B). By 4 days postfertilization (dpf) (96 hpf), the liver is in the growth phase. A left lateral view of the embryo shows the liver overlying the anterior portion of the remaining yolk ball and the anterior edge of the liver in contact with the pericardial cavity (Fig. 3C).

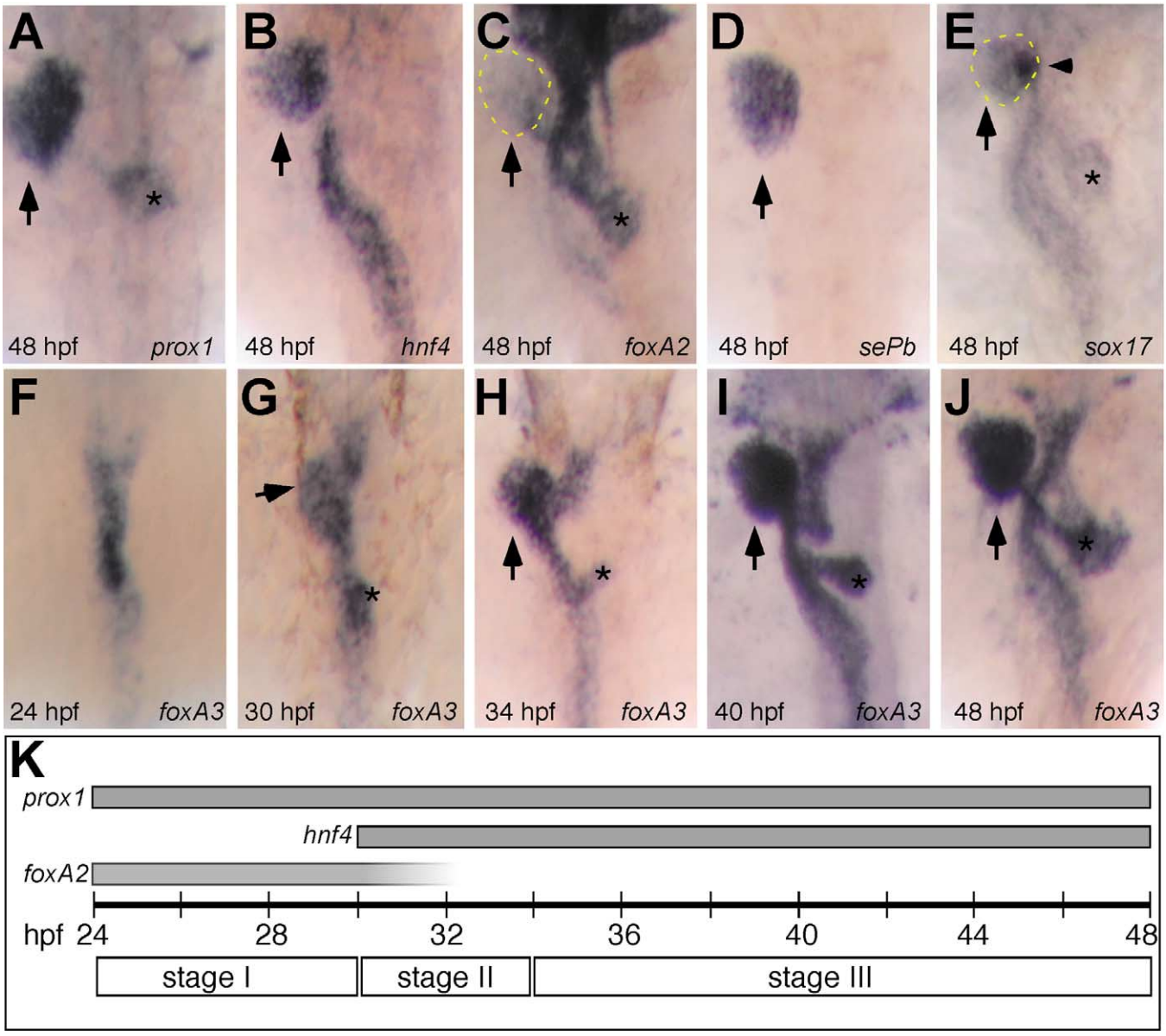

Fig. 4. Gene expression patterns in the developing digestive system. Dorsal views, anterior to the top. The liver is marked with an arrow (A–J) and outlined in yellow (C, E). The pancreas is marked with an asterisk. (A–E) Embryos are 48 hpf. (A) The level of *prox1* expression is high in the liver, slightly lower in the pancreas (asterisk), and even lower throughout the ducts connecting the two organs to the alimentary canal. (B) *hnf4* expression is restricted to the liver and alimentary canal posterior to the hepatic duct. (C) *foxA2* expression is present in the digestive system from the pharynx to the anterior boundary of the posterior intestine. Expression is highest in the pharynx, oesophagus, the endodermal lining of the swim bladder, the pancreas (asterisk) and its duct, and the ductwork of the liver. (D) *sePb* is expressed exclusively in the liver. (E) *sox17* expression is found at a low level throughout the digestive system and at a higher level in a patch of cells (arrowhead) most likely representing the gall bladder precursors. (F–J) *foxA3* expression at 24 (F), 30 (G), 34 (H), 40 (I), and 48 hpf (J); it reveals structures corresponding to those observed by fluorescence in the gutGFP line, namely the digestive system and the endodermal lining of the swim bladder. (K) Timeline showing the onset and duration of transcription factor gene expression in the liver during budding. Approximate periods of the stages of liver budding are represented under the timeline.

Gene expression in the digestive system

To identify genes that may be involved in the morphological transitions described above, we performed in situ hybridization of endodermally expressed genes at multiple time points between 24 and 48 hpf. Although the general expression pattern of these genes has been previously reported (see Materials and methods), we present them here specifically in the context of the developing digestive system. Interestingly, we found that some genes appear to initiate or halt their expression at specific morphological transitions during liver development. For example, *prox1* (Glasgow and Tomarev, 1998) expression first appears in the liver around 24 hpf, concurrent with the onset of the first stage of budding, while initiation of *hnf4* (Kudoh et al., 2001) expression appears to coincide with the onset of stage II.

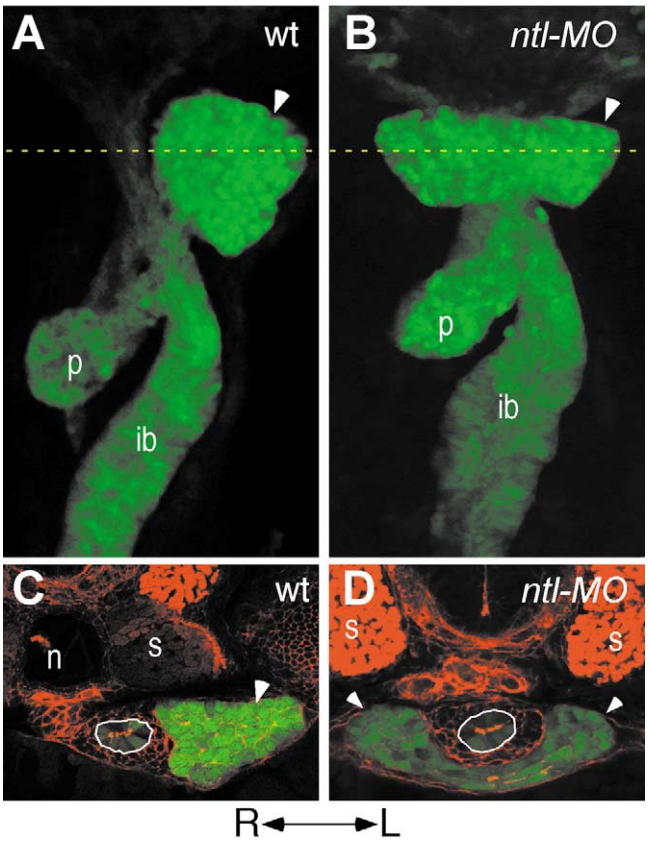

Fig. 5. The direction of liver budding can be uncoupled from the direction of intestinal bulb looping. (A, B) Ventral views of confocal stacks, anterior to the top, showing wildtype (A) and *ntl* morpholino-injected embryos (B) at 52 hpf. (A) The liver (arrowhead) in wildtype embryos is located to the left of the midline, and the intestinal bulb (ib) curves to the left. (B) In *ntl* morpholino-injected embryos where the intestinal bulb (ib) curves to the left, a single liver (arrowhead) can be located symmetrically across the midline. (C, D) Transverse sections through the gutGFP line stained with rhodamine-labeled phalloidin to visualize surrounding tissues. The liver is marked by an arrowhead; the oesophagus is outlined in white. Dorsal is to the top, and left is to the right. The level of the sections in wildtype (C) and *ntl* morpholino-injected embryos (D) is indicated by the yellow dashed lines in (A) and (B), respectively. These figures clearly show that, in *ntl* morpholino-injected embryos, the liver can reside symmetrically with respect to the midline even when the intestinal bulb loops correctly.

Initial *prox1* expression appears at the level of the first somite in a subset of medial endodermal cells that will bud to form the liver (data not shown). *prox1* expression persists throughout liver development (Fig. 4A and K). From its onset of expression, *hnf4* is found in the liver bud and the intestinal primordium posterior to the oesophagus, and this pattern of expression is observed throughout the budding process (Fig. 4B and K). Endodermal *foxA2* expression first appears by the 10-somite stage (Odenthal and Nüsslein-Volhard, 1998). By 24 hpf, *foxA2* expression stretches from the rostral end of the digestive system to the boundary between the intestinal bulb and posterior intestine (Odenthal and Nüsslein-Volhard, 1998). Shortly after the onset of budding stage II, *foxA2* expression in the liver decreases, and it is nearly absent from this organ at 32 hpf (Fig. 4K). At 48 hpf, *foxA2* expression is elevated in the hepatic and pancreatic ducts, pancreas, swim bladder, oesophagus, and pharynx, and is very low in other parts of the digestive tract (Fig. 4C).

To extend the set of molecular markers valuable to the study of the zebrafish digestive system, we also examined the expression pattern of *selenoprotein Pb (sePb)* (Kryukov and Gladyshev, 2000; Kudoh et al., 2001) and *sox17* (Alexander and Stainier, 1999), which are restricted to specific tissues. Expression of *sePb*, which encodes a serum protein produced by the liver, is first detected during stage II of liver budding and is restricted to the liver throughout the budding process (Fig. 4D). At 48 hpf, expression of *sox17* is detected at a low level throughout the digestive system with heightened expression in a subset of liver cells adjacent to the hepatic duct (Fig. 4E). In *Xenopus*, *sox17α* expression is down-regulated in all but the gallbladder (Zorn and Mason, 2001), suggesting that the cells with heightened *sox17* expression in zebrafish may also represent the gallbladder precursors.

foxA3 (Odenthal and Nüsslein-Volhard, 1998) expression is detected in the digestive tract throughout the duration of liver budding (Fig. 4F–J). The expression pattern of *foxA3* nearly mimics that of GFP in the gutGFP line, with the exclusion of pharyngeal expression, and provides a valuable alternative for visualizing the morphology of the digestive system in fixed embryos. Using this marker, liver development, as well as the development of other endodermally derived organs, can be clearly examined in the context of the digestive system.

Uncoupling the left/right positioning of the liver and intestinal bulb

Chin et al. (2000) reported that, in *no tail (ntl)* mutant embryos, liver primordia could not be detected at 30 hpf by looking at *gata6* expression, prompting us to further investigate the role of *ntl* in liver formation. In order to visualize the liver in the context of the entire digestive system, we injected *ntl* morpholino into the gutGFP line. We found that 95% of the morpholino-injected embryos perfectly phenocopied *ntl* mutants as assessed morphologically (data not shown), consistent with what has been previously reported (Feldman and Stemple, 2001). Surprisingly, we observed a distinct liver in all embryos showing *ntl* phenocopy, indicating that the liver does form, but may not differentiate properly, in embryos lacking Ntl.

In addition, we noticed that the position of the liver in Ntl-deficient embryos did not always correlate with the chirality of the intestinal bulb. Although uncoupled laterality has been observed between structures in different organ systems, such as the heart and gut (Bisgrove et al., 2000; Schilling et al., 1999), altered situs of organs within a single organ system has not been reported in zebrafish. We further investigated this phenomenon of uncoupled digestive organ position by recording the position of the liver in embryos

where the intestinal bulb had looped to either the left or right. We observed that, at 52 hpf, the intestinal bulb of 72.6% of the embryos showing a *ntl* phenotype ($n = 124$) had looped to either the left or right. [The intestinal bulbs of the other 27.4% had remained midline.] Of the 90 embryos that showed intestinal bulb looping, 65 (72%) exhibited a liver that stretched to both the left and right of the midline with a single hepatic duct connecting it to the alimentary canal (Fig. 5B and D), while the rest showed a liver that overlapped the midline but usually budded off the outer curvature of the intestinal bulb (data not shown). We observed the same phenotypes in *ntl* mutant embryos stained for *foxA3* expression (data not shown). These data show that, in the absence of Ntl, the directional outgrowth of the liver can be uncoupled from the direction of intestinal bulb looping.

Role of endothelial cells in liver budding morphogenesis

The adult liver is a highly vascularized organ, and this vascularization is critical for liver function. Recent work in mouse has indicated that endothelial cells are additionally required for liver morphogenesis, even before a vascular network is formed (Matsumoto et al., 2001). These studies showed that, in *Vegfr2/Flk-1* mutant mice, which lack endothelial cells, liver budding fails to occur altogether. Here, we investigate whether liver budding in zebrafish is also dependent on endothelial cells.

To examine the timing and nature of liver vascularization in zebrafish, we performed a time course of vascular development in the liver using the Tie2-GFP transgenic line to visualize endothelial cells (Motoike et al., 2000) and an anti-Prox 1 antibody to label the hepatocytes (Wigle et al., 1999). GFP-expressing endothelial cells are positioned adjacent to, but not completely encasing, the liver bud at 36 (data not shown) and 48 hpf (Fig. 6A). By 60 hpf, endothelial cells remain present around the liver as seen earlier, but are also found between surface hepatocytes of the liver (Fig. 6B). By 72 hpf, endothelial cells permeate the entire liver (Fig. 6C).

To analyze the potential role of endothelial cells in liver morphogenesis, we examined liver formation in embryos homozygous for the *cloche (clo)* mutation, which appear to lack all endothelial cells from an early stage (Liao et al., 1997; Stainier et al., 1995; Thompson et al., 1998). Liver budding and differentiation are indistinguishable in *clo* mutant embryos and their wildtype siblings, as assessed by *foxA3* ($n = 56$) (Fig. 6D and E) and *sePb* expression ($n = 48$) at 48 hpf (Fig. 6F and G). [*clo* mutant embryos were distinguished from their wildtype siblings by their distinct heart phenotype.] These observations suggest that, in zebrafish, endothelial cells are not required for liver budding morphogenesis or hepatocyte differentiation.

Discussion

Anatomy of the zebrafish digestive system

We have analyzed the morphogenesis of the developing zebrafish liver using a unique GFP transgenic line to facilitate observations of the endoderm. While collecting data presented in this paper, we were faced with the difficulty of choosing the correct terminology. To date, there has been no convention in the nomenclature used for zebrafish digestive anatomy, resulting in multiple terms being used to identify a single structure. With the ability to observe the entire digestive tract in the gutGFP line, we took the opportunity to define a nomenclature for the digestive anatomy of the zebrafish.

Our observations suggest that the zebrafish gut is divided into the pharynx, oesophagus, intestinal bulb, and posterior intestine, as depicted in Fig. 1. This nomenclature partitions the gut based on distinct topographical characteristics. The pharynx is the region of the alimentary canal posterior to the oral opening. The oesophagus is identified as the constricted region posterior to the pharynx. The dorsal wall of the oesophagus opens into the pneumatic duct which connects to the endodermal lining of the swim bladder. Although not part of the digestive system, the lining of the swim bladder is included here to show a complete diagram of the endodermally derived organs that express GFP in the gutGFP line. The connection of the hepatic duct to the alimentary canal demarcates the caudal boundary of the oesophagus.

The region of the digestive tract posterior to the hepatic duct has had multiple designations. It has been referred to as the stomach, the duodenum, the anterior intestine, and the foregut. The term foregut usually refers to the region of the digestive system rostral to the hepatic duct. Histological studies have been performed on both the adult and developing zebrafish digestive tract (Pack et al., 1996), and identity of this region is not exclusively analogous to the stomach or small intestine. Members of the *Cyprinidae* family, which includes zebrafish, lack stomachs, and the widened anterior portion of the intestine is referred to as the pseudogaster (Harder, 1975). However, we employed the term “intestinal bulb” to label this structure since it had previously been used for this region in adult zebrafish (Westerfield, 1995) and more precisely describes the anatomical structure.

The intestinal bulb, distinguishable primarily by its bulbous appearance, begins to develop a lumen around 42 hpf (Horne-Badovinac et al., 2001). Increases in the diameter of this lumen, amongst other events, lead to a clearly inflated structure by 3 dpf. The intestinal bulb extends caudally to the level where the gut realigns with the midline of the embryo. Posterior to the intestinal bulb lies the posterior intestine which continues down the midline of the embryo and ends at the anal opening.

The terms foregut, midgut, and hindgut are commonly used when referring to regions along the digestive tract.

However, using this terminology in zebrafish is deceptive; many of the structures used to define these regions in other organisms (Langman and Sadler, 1985) are not present in zebrafish and thus there is no consensus for where the boundaries should be. These subdivisions have been used to label the digestive tract in other fishes, although the definition of borders between regions in those organisms is again ambiguous (Harder, 1975). Given this confusion in precise anatomical terminology, we suggest that this vocabulary be used very carefully in zebrafish and only in conjunction with terms that refer to the specific structures of the digestive system.

Early in development, before a hepatic duct is formed, the boundaries of the oesophagus, intestinal bulb, and posterior intestine are not as clear. When the endoderm is a solid rod of midline cells, before the liver primordium has formed, all endoderm posterior to the constricted caudal end of the pharynx can be referred to as the intestinal rod. Once the liver primordium is present, the intestinal rod can be subdivided into three regions. The oesophagus stretches from the caudal end of the pharynx to the anterior extent of the liver bud. The intestinal bulb primordium begins at the caudal end of the oesophagus. The exact border between the intestinal bulb primordium and the posterior intestine is not easy to distinguish at this stage based on anatomy alone. Careful histological analyses will be necessary to define this boundary. Further analyses of the developing digestive system in zebrafish will undoubtedly refine the terminology proposed here.

Morphological characteristics separate liver development into two phases

To chart the timing and location of liver morphogenesis, we performed a developmental time course using the gutGFP transgenic line, which allowed us to visualize the liver in the context of the entire digestive system.

We divided liver morphogenesis into two phases: budding and growth. Budding is the phase of liver development when the organ emerges from the intestinal rod to become a separate and distinct structure on the embryo's left. Based on different shapes of the liver throughout budding, we further divided this process into three stages. Stage I begins around 24 hpf, when we first noticed an aggregation of prehepatic cells on the ventral surface of the intestinal rod. Stage II begins once the prehepatic region is a smooth thickening projecting to the left of, but still contiguous with, the intestinal bulb primordium. Stage III begins when a furrow starts forming between the anterior edge of the liver and the adjacent oesophagus and ends when the stalk of cells connecting the liver and intestinal bulb primordium forms an ordered hepatic duct with columnar epithelial cells. The behavior of hepatocytes during the budding process was somewhat surprising when compared with that described in mammals, but consistent with that seen in other fishes. In mammals, the hepatocytes appear to dissociate from one another and migrate into the mesenchyme of the adjacent septum transversum. This process is referred to by Elias (1955) as "interstitial invasion." In sea bream, as we observed in zebrafish, interstitial invasion does not appear to occur (Guyot et al., 1995). The cells of the nascent liver are closely juxtaposed, forming a single mass on the left side of the digestive tract.

The growth phase follows the completion of budding and is characterized by a dramatic change in liver size and shape. As a result of this growth phase, the liver comes to occupy a substantial portion of the abdominal cavity and spreads across the midline. Further analysis of this phase will be extremely informative since it is during this time that the liver becomes vascularized and presumably begins its physiological functions.

In addition to this detailed analysis of liver morphogenesis, we also examined the spatiotemporal expression patterns of specific molecular markers. The expression patterns of the transcription factor genes *foxA2*, *prox1*, and *hnf4* appear to correlate with stages of liver budding as defined by the morphological criteria and may represent part of the molecular network necessary for these stages to proceed. For example, *prox1* expression is initiated at the onset of stage I, consistent with data in the mouse showing a requirement for this gene in the migration of hepatocytes into the surrounding mesenchyme (Sosa-Pineda et al., 2000). *hnf4*, whose expression is initiated at the onset of stage II, has also been implicated in liver development in mouse (Li et al., 2000). Of course, there may be other molecular transitions that do not correspond to overt morphogenetic differences. These presently unobservable transitions may be identifiable through mutational analysis, and we are currently undertaking a forward genetic screen, using the gutGFP line, to identify genes regulating liver morphogenesis. Therefore, by keeping the definition of developmental phases broad at this time, we leave open the possibility of further subdividing the process of liver morphogenesis as mutant analysis uncovers additional critical transitions during liver budding and growth.

Left/right asymmetry of the liver can be uncoupled from the direction of intestinal bulb looping

The relationship between intestinal bulb chirality and the direction of liver budding has not been previously analyzed. We observed that, in wildtype liver morphogenesis, the direction of liver budding and that of intestinal bulb looping are correlated, resulting in both organs being positioned on the embryo's left. In naturally occurring cases of reversed chirality of the intestinal bulb (observed in approximately 0.1-1% of wildtype embryos, depending on the genetic background), the liver always buds off the outer curvature of the intestinal bulb primordium (unpublished observations). These observations have led to the hypothesis that the direction of liver outgrowth is dictated by the direction of looping of the intestinal bulb primordium.

Surprisingly, we found that, in the absence of Ntl, the

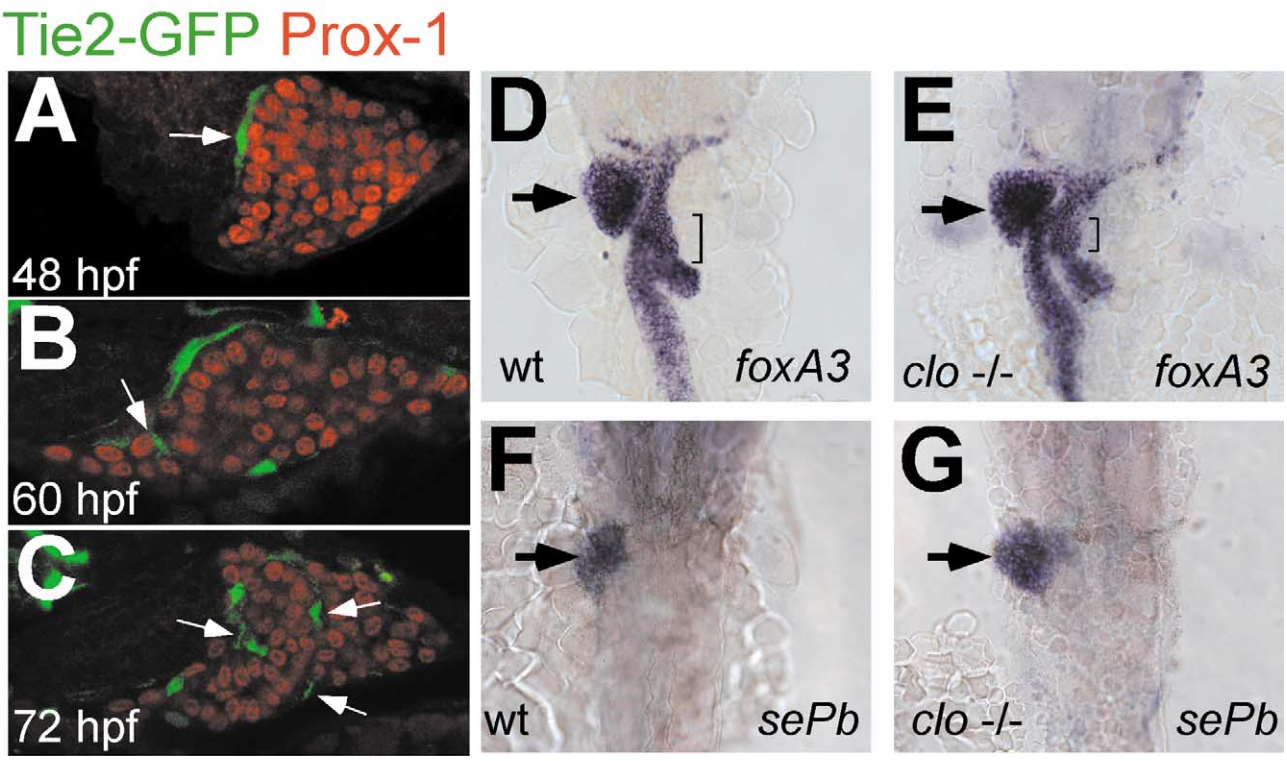

Fig. 6. Endothelial cells during liver development. (A–C) Transverse sections through Tie2-GFP transgenic embryos stained with anti-Prox1 antibody (red) to visualize hepatocytes. Dorsal is to the top, and left is to the right. (A) At 48 hpf, endothelial cells (green, arrow) line the periphery of the liver (red). (B) By 60 hpf, endothelial cells (arrow) have started to invade the liver, but are restricted to the outer edges of the liver. (C) At 72 hpf, endothelial cells (arrows) are interspersed throughout the liver. (D, E) In situ hybridization for *foxA3* expression at 48 hpf. Dorsal views, anterior to the top. The liver (arrow) of the wildtype sibling (D) and a representative *clo* mutant embryo (E) are indistinguishable. The length of the swim bladder (bracket) is variably shorter in *clo* mutant embryos. (F, G) In situ hybridization for *sePb* expression at 48 hpf. Dorsal views, anterior to the top. *sePb* expression in liver (arrow) is indistinguishable between wildtype sibling (F) and a representative *clo* mutant embryo (G).

directions of intestinal bulb looping and liver budding are frequently uncoupled; the intestinal bulb usually loops but the liver fails to bud exclusively to the left or right. The opposite phenotype has been observed in *hands-off* mutant embryos in which the intestinal bulb does not loop, yet the liver usually buds to the left or right (Sally Horne-Badovinac, E.A.O., and D.Y.R.S., unpublished observations). These data indicate that the behavior of the liver primordium is not dictated by the orientation of the intestinal bulb primordium and that the morphogenetic movements of these two organs are separable. Furthermore, these results suggest a role for the midline in the proper placement of the liver, and it will be most interesting to further investigate the mechanisms that regulate the directionality of liver budding.

Endothelial cells do not appear to be essential for liver budding morphogenesis in zebrafish

It has been reported recently that endothelial cells are required for liver budding in mouse (Matsumoto et al., 2001). Before investigating the role of endothelial cells in zebrafish liver morphogenesis, we first wanted to determine the timing and nature of endothelial/hepatic associations. We found that endothelial cells are closely associated with the liver periphery by 36 hpf and that they maintain this close apposition until approximately 60 hpf, when they begin to invade the outer layers of hepatocytes. These endothelial cells are likely part of nascent branches from the subintestinal vessels and will eventually form the hepatic vasculature (Isogai et al., 2001). By 72 hpf, endothelial cells are found throughout the entire liver, leading us to conclude that vascularization of the zebrafish liver is achieved by endothelial invasion after budding is complete. This process of vascularization appears to be different from that classically reported in mouse, where hepatocytes undergo interstitial invasion of the adjacent mesenchyme and arrange themselves around the vascular network already present (Elias, 1955).

In *Vegfr2/Flk-1*$^{-/-}$ mouse embryos, which lack mature endothelial cells, the liver never progresses beyond an early thickening of hepatic endoderm on the gut tube (Matsumoto et al., 2001). The zebrafish *clo* mutation, which appears to disrupt endothelial cell differentiation at a stage upstream of *Vegfr2/Flk-1* expression (Liao et al., 1997; Thompson et al., 1998), provides a tool in zebrafish for studying the behavior of hepatocytes in the apparent absence of endothelial cells. If the primary conserved role of endothelial cells in liver development is to initiate morphogenesis, one would expect

the liver of *clo* mutant embryos to arrest during stage I of budding. We performed a qualitative analysis of the size and shape of the liver in *clo* mutant embryos. Surprisingly, liver budding and differentiation in *clo* mutant embryos appear to proceed normally. The discrepancy of these findings with those described in *Vegfr2/Flk-1*$^{-/-}$ mouse embryos may be explained in several ways, including by a difference in cell behavior during liver outgrowth between these species. One possibility is that signals from the endothelial cells may be necessary for the breakdown of cell adhesion between hepatocytes. In mouse, this function would be concomitant with initiation of hepatocyte migration. However, since cell dissociation does not occur in zebrafish liver morphogenesis, the presence of endothelium would be dispensable for budding. This model would suggest that the growth phase, during which endothelial cells invade the liver, may be affected in *clo* mutant embryos. However, due to an increased severity of the cardiac edema, we were not able to analyze these later time points. An alternative explanation for the discrepancy between mouse and zebrafish is that signals provided by the endothelial cells in mouse may be produced by a different cell type in zebrafish. Other explanations are of course possible.

The zebrafish has the potential to contribute significantly to studies of the vertebrate digestive system. With its proven usefulness for large-scale forward genetics screens and embryological studies, and with the addition of the gutGFP line, we hope that this model organism will become invaluable to investigate the molecular and cellular mechanisms of endodermal organ development.

Acknowledgments

We would like to thank Steve Waldron for expertly maintaining the zebrafish stocks; Herwig Baier for the invaluable gift of the gutGFP zebrafish line; Juan Engel and the UCSF Liver Center for training and assistance on the confocal microscope; Guillermo Oliver for the generous gift of anti-Prox1 antibody; Tetsuhiro Kudoh and Michael Tsang for sharing plasmids encoding Selenoprotein Pb and Hnf4 before publication; Peter Chien, Sally Horne-Badovinac, Matthias Hebrok, Karen Borst-Rothe, and the Stainier lab for discussion and critical comments on the manuscript. E.A.O. was supported by an AHA fellowship. This work was supported in part by grants from the NIH (NIDDK) and the Packard Foundation (to D.Y.R.S.).

References

Alexander, J., Stainier, D.Y., 1999. A molecular pathway leading to endoderm formation in zebrafish. Curr. Biol. 9, 1147–1157.

Alexander, J., Stainier, D.Y., Yelon, D., 1989. Screening mosaic F1 females for mutations affecting zebrafish heart induction and patterning. Dev. Genet 22, 288–299.

Biemar, F., Argenton, F., Schmidtke, R., Epperlein, S., Peers, B., Driever, W., 2001. Pancreas development in zebrafish: early dispersed appearance of endocrine hormone expressing cells and their convergence to form the definitive islet. Dev. Biol. 230, 189–203.

Bisgrove, B.W., Essner, J.J., Yost, H.J., 2001. Multiple pathways in the midline regulate concordant brain, heart and gut left–right asymmetry. Development 127, 3567–3579.

Cascio, S., Zaret, K.S., 1991. Hepatocyte differentiation initiates during endodermal–mesenchymal interactions prior to liver formation. Development 113, 217–225.

Chin, A.J., Tsang, M., Weinberg, E.S., 2001. Heart and gut chiralities are controlled independently from initial heart position in the developing zebrafish. Dev. Biol. 227, 403–421.

Edlund, H., 2002. Pancreatic organogenesis: developmental mechanisms and implications for therapy. Nat. Rev. Genet. 3, 524–532.

Elias, H., 1955. Origin and early development of the liver in various vertebrates. Acta Hepatol. 1–57.

Feldman, B., Stemple, D.L., 2001. Morpholino phenocopies of *sqt, oep,* and *ntl* mutations. Genesis 30, 175–177.

Gualdi, R., Bossard, P., Zheng, M., Hamada, Y., Coleman, J.R., Zaret, K.S., 1996. Hepatic specification of the gut endoderm in vitro: cell signaling and transcriptional control. Genes Dev. 10, 1670–1682.

Glasgow, E., Tomarev, S.I., 1998. Restricted expression of the homeobox gene *prox 1* in developing zebrafish. Mech. Dev. 76, 175–178.

Guyot, E., Diaz, J.P., Connes, R., 1995. Organogenesis of the liver in sea bream. The Fisheries Society of the British Isles 47, 427–437.

Harder, W., 1975. Anatomy of Fishes. Schweizerbart, Stuttgart.

Heasman, J., Kofron, M., Wylie, C., 2000. Beta-catenin signaling activity dissected in the early *Xenopus* embryo: a novel antisense approach. Dev. Biol. 222, 124–134.

Horne-Badovinac, S., Lin, D., Waldron, S., Schwarz, M., Mbamalu, G., Pawson, T., Jan, Y., Stainier, D.Y., Abdelilah-Seyfried, S., 2001. Positional cloning of *heart and soul* reveals multiple roles for PKCλ in zebrafish organogenesis. Curr. Biol. 11, 1492–1502.

Isogai, S., Horiguchi, M., Weinstein, B.M., 2001. The vascular anatomy of the developing zebrafish: an atlas of embryonic and early larval development. Dev. Biol. 230, 278–301.

Jung, J., Zheng, M., Goldfarb, M., Zaret, K.S., 1999. Initiation of mammalian liver development from endoderm by fibroblast growth factors. Science 284, 1998–2003.

Krauss, S., Johansen, T., Korzh, V., Moens, U., Ericson, J., Fjose, A., 1991. Zebrafish pax[zf-a]: a paired box-containing gene expressed in the neural tube. EMBO J. 10, 3609–3619.

Kryukov, G.V., Gladyshev, V.N., 2000. Selenium metabolism in zebrafish: multiplicity of selenoprotein genes and expression of a protein containing 17 selenocysteine residues. Genes Cells 5, 1049–1060.

Kudoh, T., Tsang, M., Hukriede, N.A., Chen, X., Dedekian, M., Clarke, C.J., Kiang, A., Schultz, S., Epstein, J.A., Toyama, R., Dawid, J.B., 2001. A gene expression screen in zebrafish embryogenesis. Genome Res. 11, 1979–1987.

Langman, J., Sadler, T.W., 1985. Langman's Medical Embryology. Williams & Wilkins, Baltimore.

Le Douarin, N.M., 1970. Induction of determination and induction of differentiation during development of the liver and certain organs of endomesodermal origin, in: Wolff, E. (Ed.), Tissue Interactions during Organogenesis, Gordon and Breach, New York, pp. 37–70.

Le Douarin, N.M., 1975. An experimental analysis of liver development. Med. Biol. 53, 427–455.

Li, J., Ning, G., Duncan, S.A., 2000. Mammalian hepatocyte differentiation requires the transcription factor HNF-4α. Genes Dev. 15, 464–474.

Liao, W., Bisgrove, B.W., Sawyer, H., Hug, B., Bell, B., Peters, K., Grunwald, D.J., Stainier, D.Y., 1977. The zebrafish gene *cloche* acts upstream of a *Flk-1* homologue to regulate endothelial cell differentiation. Development 124, 381–389.

Matsumoto, K., Yoshitomi, H., Rossant, J., Zaret, K.S., 2001. Liver organogenesis promoted by endothelial cells prior to vascular function. Science 294, 559–563.

Motoike, T., Loughna, S., Perens, E., Roman, B.L., Liao, W., Chau, T.C., Richardson, C.D., Kawate, T., Kuno, J., Weinstein, B.M., Stainier, D.Y., Sato., T.N., 2000. Universal GFP reporter for the study of vascular development. Genesis 28, 75–81.

Odenthal, J., Nüsslein-Volhard, C., 1998. fork head domain genes in zebrafish. Dev. Genes Evol. 208, 245–258.

Pack, M., Solnica-Krezel, L., Malicki, J., Neuhauss, S.C.F., Schier, A.F., Stemple, D.L., Driever, W., Fishman, M.C., 1996. Mutations affecting development of zebrafish digestive organs. Development 123, 321–328.

Reimold, A.M., Etkin, A., Clauss, I., Perkins, A., Friend, D.S., Zhang, J., Horton, H.F., Scott, A., Orkin, S.H., Byrne, M.C., Grusby, M.J., Glimcher, L.H., 2000. An essential role in liver development for transcription factor XBP-1. Genes Dev. 14, 152–157.

Rossi, J.M., Dunn, N.R., Hogan, B.L., Zaret, K.S., 2001. Distinct mesodermal signals, including BMPs from the septum transversum mesenchyme, are required in combination for hepatogenesis from the endoderm. Genes Dev. 15, 1998–2009.

Schilling, T.F., Concordet, J., Ingham, P.W., 1999. Regulation of left–right asymmetries in the zebrafish by *Shh* and *BMP4*. Dev. Biol. 210, 277–287.

Slack, J.M., 1995. Developmental biology of the pancreas. Development 121, 1569–1580.

Sosa-Pineda, B., Wigle, J.T., Oliver, G., 2000. Hepatocyte migration during liver development requires Prox 1. Nat. Genet. 25, 254–255.

Stainier, D.Y., Weinstein, B.M., Detrich, H.W., 3rd, Zon, L.I., Fishman, M.C., 1995. *cloche*, an early acting zebrafish gene, is required by both the endothelial and hematopoietic lineages. Development 121, 3141–3150.

Stainier, D.Y., 2001. Zebrafish genetics and vertebrate heart formation. Nat. Rev. Genet. 2, 39–48.

Thisse, C., Zon, L.I., 2002. Organogenesis: heart and blood formation from the zebrafish point of view. Science 295, 457–462.

Thompson, M.A., Ransom, D.G., Pratt, S.J., MacLennan, H., Kieran, M.W., Detrich, H.W., 3rd, Vail, B., Huber, T.L., Paw, B., Brownlie, A.J., Oates, A.C., Fritz, A., Gates, M.A., Amores, A., Bahary, N., Talbot, W.S., Her, H., Beier, D.R., Postlethwait, J.H., Zon, L.I., 1998. The *cloche* and *spadetail* genes differentially affect hematopoiesis and vasculogenesis. Dev. Biol. 197, 248–269.

Westerfield, M., 1995. The Zebrafish Book: A Guide for the Laboratory Use of Zebrafish (*Danio rerio*). M. Westerfield, Eugene, OR.

Wigle, J.T., Chowdhury, K., Gruss, P., Oliver, G., 1999. *Prox1* function is crucial for mouse lens-fibre elongation. Nat. Genet. 21, 318–322.

Zaret, K.S., 2002. Regulatory phases of early liver development: paradigms of organogenesis. Nat. Rev. Genet. 3, 499–512.

Zorn, A.M., Mason, J., 2001. Gene expression in the embryonic *Xenopus* liver. Mech. Dev. 103, 153–157.